On the long-term correlations in the twinning and dislocation slip dynamics

E. Agletdinov[1], D. Drozdenko[2,3], P. Harcuba[2], P. Dobron[2], D. Merson[1] and A. Vinogradov[4]

[1]Institute of Advanced Technologies, Togliatti State University, Togliatti, 445020, Russia

[2]Faculty of Mathematics and Physics, Charles University, 121 16 Prague, Czech Republic

[3]Magnesium Research Center, Kumamoto University, Kumamoto, 860-8555 Japan

[4]Department of Mechanical and Industrial Engineering, Norwegian University of Science and Technology – NTNU, Trondheim 7491, Norway

The present work aims at gaining new insights into the dynamics of the dislocation slip and twinning processes, which govern the majority of possible scenarios of plastic deformation in structural metals and alloys. Using model magnesium single crystals and employing the statistical analysis of acoustic emissions (AE) generated in the course of plastic deformation, it was demonstrated that twinning is a process with a memory of the past whereby the twinning events affect the occurrence of successive events. As opposes to this, the basal dislocation slip appears as a substantially random intermittent process comprising of independent elementary slip events without long-term correlations between gliding dislocations or slip bands emerging due to the collective dislocation glide along basal planes. The single crystals were chosen with axial orientations best suitable to facilitate either basal dislocation slip or tensile twinning under compressive loading, which significantly simplified the interpretations of AE findings. Besides, the AE results were fully corroborated *in situ* by microstructure observations using scanning electron microscopy imaging.

Keywords: mechanical twinning; dislocation slip; acoustic emission; magnesium; single crystal

1. Introduction: motivation and methodology

Deformation twinning is a displacive transition which occurs by high-speed collective displacements of a large number of atoms across many scales in space and time [1, 2]. In time, the mechanical twinning may evolve through several stages involving nucleation of tiny embryos and their coalescence before the twin nucleus shoots through a perfect crystal as a propagating lamella [3]. Using temporal statistical analysis of the acoustic emission (AE) time series acquired during tensile deformation of the polycrystalline magnesium alloy ZK60, some of the present authors [4] have demonstrated recently that the mechanical twinning belongs to a wide class of non-Poisson random processes. In other words, twinning manifests itself as a process with a memory of the past. The alloy ZK60 is a typical hexagonal close-packed (hcp) metal exhibiting strain hardening which involves the activation and interplay between the dislocation slip and twinning – the two primary deformation mechanisms for many hcp metals and alloys. The concurrent operation of these mechanisms substantially complicates the analysis and the interpretation of the results. In particular, the highly possible dislocation-twin interactions, which are common in deformed polycrystalline hcp magnesium [2, 5-8], could affect the conclusions drawn in [4]. To separate these deformation mechanisms and eliminate the short-term slip-twin interactions, the use of a properly oriented single crystal is indispensable [9, 10]. Single crystals of magnesium are highly anisotropic due to the large difference in critical resolved shear stress (CRSS) for the deformation systems, that makes the activation of deformation mechanisms predictable and controllable. Therefore, to validate the methodological approach proposed in [4], in the present work, a comparative analysis was made of the temporal structure of the AE time series arising in magnesium single crystals where either dislocation slip or deformation-induced twinning were promoted as dominant deformation modes during compression loading. Specifically, the compression along the axis $\langle 11\bar{2}2 \rangle$ is associated with the prevalence of the basal <a> slip having the highest Schmid factor of 0.5, while the compression along the $\langle 11\bar{2}0 \rangle$ axis triggers extension twinning as the primary deformation mode. The detailed statistical AE analysis was corroborated by the *in situ* secondary electron (SE) imaging providing insight into the microstructure evolution during loading.

2. Materials and Methods

2.1. Materials and testing

The magnesium single crystals (of 99.95% commercial purity) were grown by a modified vertical Bridgman technique from monocrystalline seeds. The specimens (of $5 \times 5 \times 6$ mm^3) specifically oriented for uniaxial compression along the $\langle 11\bar{2}2 \rangle$ axis or the $\langle 11\bar{2}0 \rangle$ axis to promote either basal

slip or twinning, respectively, were prepared from the as-cast ingots by spark erosion. The desired initial orientation of the specimens was confirmed by means of X-ray diffraction (Panalytical X-ray $\theta–2\theta$ diffractometer, CuK$_\alpha$ radiation).

The mechanical loading, accompanied by AE measurements, was performed using the Instron 5882 universal testing machine at the constant nominal strain rate of 10^{-3} s^{-1} at room temperature.

The AE activity was monitored by a computer-controlled setup based on the PCI-2-based (Physical Acoustic Corporation) board operating in a continuous thresholdless mode with 2 MHz sampling frequency. The sensor - a miniature piezoelectric transducer MST8S (Dakel-ZD Rpety, Czech Republic) having a diameter of 3 mm and a reasonably flat response in the 100-600 kHz frequency range - was attached to the holder in close proximity to the specimen. The signal was pre-amplified by 40 dB before an acquisition. The full scale of the A/D converter used in the acquisition chain was ±10 V providing the total dynamic range of 100 dB. The background input noise during the tests did not exceed 10 μV peak-to-peak. Details of the AE signal processing are given in the following sub-sections.

To verify the outcomes of the indirect AE analysis and to provide a deeper insight into the microstructure evolution during compressive deformation of magnesium single crystals, the *in situ* scanning electron microscopy (SEM) imaging, using secondary and backscattered electron detection, was performed in the chamber of the filed-emission scanning electron microscope Zeiss Crossbeam Auriga equipped with the deformation stage MTEST Quattro (Materials Testing system ADMET). The *in situ* deformation tests were periodically paused for obtaining the SEM images of the surface morphology at different strains and magnifications. Prior to observations, the surface was ground and polished using a diamond paste down to the ¼ µm grade, and, finally, electrolytically polished using the Struers Lectropol in AC2 electrolyte at 18 V, -40°C for 30 s.

2.2. AE analysis of arrival times of event in time series

AE resulting from localised sources due to rapid stress relaxation in the solids resembles seismic time series and appears as a set of electric pulses at the sensor output as is illustrated in Fig. 1 representing the different typical fragments of the AE behaviour observed in the Mg single crystals tested in the present work. Following the data processing strategy proposed in [4] for the assessment of possible correlations in the behaviour of deformation-induced defects, the AE time series reduces to a point process which is characterised solely by a set of arrival times of events $\left\{ t_0,\ t_1 \ldots t_i \ldots t_N \right\}$ shown schematically by dashed lines in Fig. 1b, d. In practice, it is more convenient to investigate the distribution of time intervals or inter-arrival times between the

successive events $\Delta t_i = t_{i+1} - t_i$, c.f. Fig. 1b, d. Assuming that the sources of local stress relaxation resulting in the AE events are independent, a Poisson-type time series [11] is anticipated in the form of a train of Dirac's δ-impulses $\delta(t - t_k)$ with amplitudes U_k

$$A(t) = \sum_{k=1}^{N} U_k \delta(t - t_k) \tag{1}$$

The inter-arrival time intervals Δt_i should, therefore, obey an exponential distribution with the probability density function (PDF)

$$\rho(\Delta t) = \frac{1}{\overline{\Delta t}} \exp(-\Delta t / \overline{\Delta t}) = \lambda \exp(-\lambda \Delta t) \tag{2}$$

where $\overline{\Delta t}$ is the average time interval between the pulses in a time-series (averaging is done over the time interval T) and $\lambda = 1 / \overline{\Delta t}$ is the average intensity (also termed as count rate or activity) of the pulse flow on the chosen time interval T.

Since the properties of any random process are fully determined by the PDF of the descriptive random variable, the AE stream was sectioned into a set of successive realisations and the PDF $\rho(\Delta t)$ was obtained for each *j-th* realisation. The statistical goodness-of-fit χ^2 test was applied to probe the agreement between the inter-arrival times Δt and the Poisson distribution (2) with the count rate $\lambda_j = N_j / T$ for each realisation $j \in [1, K]$.

2.3. Non-supervised cluster analysis of AE data

In magnesium polycrystals with typical grain sizes in the ten-micrometre range and above, the main deformation mechanisms - dislocation slip and twinning - co-exist in the course of plastic deformation. As opposes to this and as discussed above, the contributions from both mechanisms are well-separated in the deformation history of the suitably oriented single crystals. The dislocation motion along the slip planes and twinning differ significantly in their source dynamics and, therefore, they generate AE with different waveforms (low-amplitude waveforms fluctuating in a wider range of frequencies, which are produced by dislocation slip, can be compared to high amplitude transients for twinning [12, 13]). To discriminate quantitatively between the sources of different origin in random AE time series, the proposed by Pomponi and Vinogradov *adaptive sequential k-means* (ASK) signal clusterisation algorithm [14] has been proven effective. For the cluster analysis, the acquired AE stream was sectioned into successive realisations of 4096 samples. The Fourier power spectral density (PSD) function was calculated for each realisation by the Welch technique and normalised to unite area for comparison. The ASK procedure groups together the signals with similar PSDs while disjoins the signals having statistically different spectra. The symmetrical version of the Kullback-Leibler distance is used in the present work as a measure of

similarity/dissimilarity between normalised PSDs (see [12, 15-17] for mathematical details and implementation of the ASK algorithm and illustrative case studies).

3. Results and data analysis

3.1. Statistical analysis of arrival times in AE time series

Raw streaming AE data (coloured in grey) superimposed with the loading curves are shown in Figs. 2 and 3 in parallel with the main results of the statistical analysis of AE time series. The coloured symbols depict the count rate λ, i.e. the number of detected events per unit time, of the AE flow, calculated for statistically representative samples of the time series. The colour of the symbol corresponds to the result of the Pearson's test for each sample: the green coloured triangles correspond to the fragments of the AE stream where the distribution of the inter-arrival times agrees with the exponential Poisson distribution, Eq.(2), while the red colour marks the sections with the non-Poisson behaviour of the sources. In other words, the green colour denotes the samples with the Poisson process of random and independent events, while the red colour indicates the samples with a statistically significant deviation from the Poisson process, which heralds the existence of a temporal correlation between the events in the time series. The AE pulse flow is intense in both specimens tested. On the time scale shown in Figs. 2 and 3, the AE stream looks like a continuous noise signal which never vanishes in the entire interval of observation. However, on the smaller time scales, AE for both specimens tested appears as pulse trains consisting of well-separated transients of different amplitudes as has been clearly illustrated in Fig. 1 showing typical fragments of AE time series corresponding to green- (a,b) and red- (c,d) coloured fragments (Poisson and non-Poisson, respectively) of the AE activity shown in Fig. 3 for the magnesium single crystal deformed along the $\langle 11\bar{2}0 \rangle$ axis. The arrival times for each transient including those with the low signal-to-noise ratio, c.f. small transients shown in Fig. 1c, were picked using the algorithm described in [18, 19]. Typical experimental histograms of the waiting time distributions, i.e. the probability density functions of the inter-arrival times, are shown in Figs. 4 and 5 for both specimens tested. Each figure consists of eight sub-plots referring to different deformation stages indicated by time marks on each sub-plot. The solid lines superimposed onto the experimental probability density histograms represent the theoretical exponential functions according to Eq.(2) , which are anticipated for the Poisson process of the same intensity λ as that obtained from the respective sample distribution (notice that these are not the fitting curves). Besides the quantitative changes in PDFs, which trivially caused by the changes in AE activity, the qualitative changes occur as reflected by the Pearson's goodness-of-fit p-test values for the experimental histogram shown on the corresponding diagrams. The p-value less than the 0.05 significance level suggests

that one cannot accept the null hypothesis stating that the data are consistent with a specified Poisson distribution and that there is a significant difference between the observed and the expected Poisson frequency.

The crystal, which is loaded in compression along the ⟨11$\bar{2}$2⟩ direction deforms mainly by basal slip. The remarkable result is that in this case the statistical AE analysis consistently shows that the dislocation slip generates acoustic emissions following the Poisson's behaviour featured by the exponential distribution of the inter-arrival times, Fig. 4. This behaviour is persistent and is observed throughout the experiment, except the very initial stage of loading, where multiple "false" AE events appeared due to initial self-adjustments and rubbing in the deformation rig at small loads, Fig. 1. Therefore, this early deformation stage was excluded from the analysis.

For the crystal ⟨11$\bar{2}$0⟩ deformed in compression, the typical initial plateau with little work hardening due to profuse tensile twinning is observed on the stress-strain curves in Fig. 3. The AE flow on this stage is particularly intense and a broad peak of the AE count rate is observed from 0 to 120 s. Within the same time interval, the χ^2 goodness-of-fit test suggests that the Poisson model does not represent the experimental data as indicated by the red symbols on the AE intensity diagram. This behaviour is at sharp contrast with what has been seen above for the ⟨11$\bar{2}$2⟩ oriented crystal and is indicative of existing temporal correlations in the spontaneous fluctuating behaviour of emitting defects. It has been proposed recently [4], that the twinning process in magnesium alloys can be regarded as a non-Poisson self-exciting process with the memory of the past. The present results obtained on suitably oriented single crystals fully corroborate this conclusion leaving no doubts that the long-term correlations are seen in the collective dynamics of twins. These should not be confused with the strong short-term avalanche-like correlations between elementary twinning dislocations forming each individual twin; these correlations are observed in the nano-and sub-microsecond range riving rise to high amplitude transient AE signals with sharp fronts and wide power spectra [20]. The distribution of the time intervals between the events, Fig. 5b-f, measured with a sub-millisecond resolution suggests further that the observed correlations are caused by the influence that twinning events exert on their nearest neighbours, as it is expected in the random self-exciting Hawkes point process [21, 22]. The essential property of the a process is that the occurrence of any event in a random sequence increased the probability of further events. Due to this feature, this process has found numerous applications in modelling the arrival of random events with the clustering/branching effect in economics, biology and many other disciplines [22]. The characteristic time scale where the remarkable deviation of the distribution of interarrival times is observed from the Poisson exponential behaviour is found to be of the order of few milliseconds or less. At the mature stage of the uniform deformation (approximately 120-

200 s), the dynamics of the AE events changes so that the transients appear to be distributed according to the Poisson model as is indicated by green triangles on the tail of the AE activity curve in Fig. 3. At this stage, the exponential (Poisson) distribution of time intervals is consistently observed, Fig. 5g and h.

Results of the statistical analysis of inter-arrival times in AE time series are supplemented by the independent characterisation of underlying mechanisms by means of the cluster analysis of the AE datasets as discussed in the following section.

3.2. Non-supervised cluster analysis of AE

Results of the application of the ASK clusterisation algorithm to the AE streaming data are summarised in terms of the number of class members accumulated during loading time as shown in Fig. 2b and 3b for both differently oriented single crystals. This procedure reveals that the AE signals fall into few primary categories (three and two for the crystals with $\langle 11\bar{2}2 \rangle$ and $\langle 11\bar{2}0 \rangle$ axial orientation, respectively) with statistically different features (the realisations corresponding to the background electrical noise, which is inevitable in the highly sensitive AE setups, were also identified and filtered out). These groups are distinct by their PSDs having different relative fractions of low and high-frequency components. The characteristic statistical features of these groups do not differ fundamentally from those discussed early for typical AE mechanisms originating from dislocation slip and twinning (see, e.g. [4, 12, 15]) – low amplitude AE signals with relatively wide and strongly fluctuating spectra are associated with dislocation activity, while the high-amplitude transients with the compact frequency distribution in the power spectra are related to the twinning dynamics.

During compression along the $\langle 11\bar{2}2 \rangle$ axis, three clusters corresponding to different AE sources have been revealed by the ASK procedure, Fig. 2b. Here and in what follows, the clusters are labelled on the first-come-first-numbered basis. Cluster 1 (green line), corresponding to the first active AE mechanism is characterised by the low amplitude AE and lower frequency components prevailing in the PSD, which is typically associated with the dominance of dislocation slip in the deformation process. One can notice, that this cluster evolves steadily throughout the test as it is reasonably expected for the basal slip active in single crystals with this orientation. Cluster 2 (red line), which comes into play notably later in the deformation history, is composed of high-frequency transient signals with high peak amplitudes, which are assumed naturally from the preponderance of mechanical twinning over slip. From the kinetics of individual clusters, which is explicit in Fig. 2b, it is obvious that this cluster progresses significantly slower compared to Cluster 1 (basal slip). Moreover, after around 170 s, this cluster does not grow any more, i.e. the associated mechanism ceases to emit elastic waves. Cluster 3 (cyan line) appears almost immediately after Cluster 2 with a

7

just slight delay, i.e. the mechanism responsible for Cluster 3 triggers shortly after several first twins show up. It then keeps growing, though one can notice that the rate of new members acquisition in this class reduces at approximately the same time as Cluster 2 saturates, thus indicating the intimate interconnection between the underlying mechanisms. Considering that features of Cluster 3 bear plenty of similarity to those of Cluster 1 assigned to dislocation slip, and Cluster 3 most likely represents the slip in the twinned regions.

The AE cluster pattern in the single crystal deformed in compression of crystal along the $\langle 11\bar{2}0 \rangle$ axis is different, Fig. 3b. In this case, the ASK procedure reveals two distinct clusters. The activated first Cluster 1 (red line) is comprised of AE signals with high peak amplitudes (similarly to Cluster 2 in the $\langle 11\bar{2}2 \rangle$ oriented crystal), and, therefore, it is most reasonably assigned to mechanical twinning. The number of members in this cluster gradually increases with strain/time before reaching saturation at approximately 120 s. At about 35 s, Cluster 2 (green line) associated with basal slip comes into play as a minor contributor to the overall AE signal. However, this cluster then evolves rapidly so that a crossover between the two modes occurs at approximately 85-90 s – exactly at the time when the inflexion point is observed on the loading diagram as indicated by the dashed line, Fig. 3a. As deformation proceeds, the dislocation slip plays a more and more significant role in the strain hardening process, and, finally, it becomes a dominant mechanism of energy dissipation and strain accommodation in the deforming crystal.

3.3. Microstructure development: *in situ* SEM imaging

The *in situ* microstructural observations fully confirm the conclusions drawn from both independent methods of AE data analysis discussed above. During compression loading of the magnesium single crystal along the $\langle 11\bar{2}2 \rangle$ axis, Fig. 6, only individual slip lines appear on the free surface along the basal plane. As deformation proceeds, those lines become more and more visible. The important difference with the deformation process in polycrystals, where the slip lines emerge randomly and independently here and there in differently oriented grains, all slip lines in the single crystal belong to the same family of basal planes. Although this axial orientation of the single crystal is theoretically "ideal" for basal slip, a few tiny $\{10\bar{1}2\}\langle 11\bar{2}2 \rangle$ extension twins are observed on the mature deformation stage at about 200 s. However, with further loading, those twins barely grow in width (c.f. the SEM image taken at 300 s), thus confirming that this orientation is not favourable for twinning. At a higher magnification, the dislocation slip lines can be resolved in the twinned regions, as is shown in the inset in Fig. 6.

In case of compression loading of the magnesium single crystal along the $\langle 11\bar{2}0 \rangle$ axis, Fig. 7, the wide $\{10\bar{1}2\}\langle 11\bar{2}2 \rangle$ extension twins can be observed already at the beginning of deformation (c.f. the SEM image taken at 25 s). These deformation twins continue growing fast

with further loading (c.f. the SEM image taken at 50 s). At 75 s after the beginning of the test, the crystal is nearly completely twinned (this was confirmed by the electron back-scattered diffraction measurements of the crystal orientation). The slip traces resulting from profuse dislocation motion become visible much later than mechanical twins (c.f. the SEM image taken at 75 s). As $\{10\bar{1}2\}\langle11\bar{2}2\rangle$ extension twinning results in the reorientation of the initial crystal lattice by 86.3º, the observed slip lines can be reasonably assigned to the basal slip in the twinned volume.

4. Discussion

Plastic deformation during compression of the magnesium crystal along the $\langle11\bar{2}2\rangle$ axis is governed by dislocation motion on basal planes. This deformation mode activates most easily due to the highest Schmid factor being of 0.5. The analysis of the AE time series unequivocally suggests that the observed long individual slip lines on the surface, Fig. 6, are detectable sources of AE associated with the collective motion of dislocations, similarly to what has been observed on even a smaller scale in locally loaded pure copper [23]. However, it should be noted that unlike what is commonly seen in pure *fcc* metals where AE appears as a continuous signal, the raw AE signal in magnesium appears to be transient regardless of whether it was generated by twins or moving dislocation, Fig. 3. It has long been understood that mechanical twinning, being a very fast process of crystal lattice re-orientation involving cooperative motion of a large number of twinning dislocations, generates very powerful high-amplitude AE bursts, which, unlike most other AE sources, can be audible: "tin cry" or "crackling" sound are well-known examples of this kind of behaviour [24]. In the present work, a few tiny tensile twins are found in the single crystals specifically oriented for basal slip. The *in situ* microstructure observations reveal them undoubtedly albeit with the notable time lag compared to AE data indicating the early appearance of twins as represented in Fig. 1b: c.f. AE – 50 s vs SEM imaging – 200 s. This time difference should not be confusing and could be explained by the complexity of the twinning process on the one hand and by the limitations of direct *in situ* observations on the other. As it has been mentioned in Section 3.2, the extension twins grow thickness-wise relatively slowly even at the mature loading stage (c.f. images taken at 200-300 s in Fig. 6). On the other hand, the AE method is sensitive to twin nucleation, while the twin thickening does not produce detectable AE due to the significant difference in the velocity of twin nucleation (propagation in length) and thickening (propagation in width) [25]. Therefore, there is a reasonably expected delay between the time of twin nucleation detected by AE and the time when the twin becomes wide enough for reliable recognition at relatively small magnifications used in the present *in situ* observations. Moreover, one should bear in mind that AE is a technique receiving information about evolving defects from

the entire specimen volume, while the SEM imaging technique is limited to the 2D field of view capturing only a fraction of the deforming surface. Therefore, the freshly nucleated twins, which are detected by AE already at 50 s, might be invisible at the surface or they are too small to be resolved under the SEM imaging conditions applied. Besides, we should underline that the statistical AE analysis strongly suggested that twinning served only as an occasional contributor to the overall AE in the magnesium crystal deformed in compression along the $\langle 11\bar{2}2 \rangle$ axis. These observations appear to be in excellent agreement with the works of Chapius and Driver [26] and Molodov et al. [27], where anomalous extension twins in plane-strain (channel-die) compressed magnesium single crystals preferentially oriented for basal slip have been observed and discussed. Besides basal slip entailing a rotation of the c-axis towards the compression direction, the twins were found parallel to the constraint in order to compensate the deformation heterogeneity with respect to the slip-induced orientation change. The twins variants formed in symmetrical pairs [27] to mutually compensate their shear components in the lateral constraint $\langle 10\bar{1}0 \rangle$ direction. The appearance of twins close to the loading platens in the present work can be reasonable for the same reason - compensation of the basal slip induced rotation of the crystal.

In sharp contrast with the behaviour of the $\langle 11\bar{2}2 \rangle$ crystal, the activation of $\{10\bar{1}2\}\langle 10\bar{1}1 \rangle$ extension twins easily occurs when the compression load is applied normally to the *c*-axis [9, 28, 29]. In this situation, the Schmid factors for the extension twinning system, prismatic and basal slip systems are of 0.5, 0.43 and 0, respectively [30]. Therefore, in the present work, extension twinning is the dominant deformation mode in the single crystals compressed along the $\langle 11\bar{2}0 \rangle$ axis. Further plastic straining of the re-oriented (twinned) grains is accommodated by the <a> dislocation slip on the basal and prismatic planes. The mechanisms predicted from the Schmid factor analysis appear in harmony with both the AE results and the *in situ* SEM observations. While the high-amplitude signals prevailing at the beginning of loading, Fig. 3a, and the ASK analysis collectively signify twinning activity indirectly, the direct *in situ* microstructure observation, Fig. 7, firmly entrenches the AE-based hypothesis and strengthens the conclusions drawn from the AE method. Furthermore, the gradual involvement of the dislocation slip as a complementary accommodation mechanism is clearly observed as the deformation proceeds beyond the inflexion point on the strain hardening curve. Once activated, dislocation slip followed by storage mediates the strain hardening process giving rise to the sigmoidal shape of the strain hardening diagram in Fig. 2.

The AE signal clustering procedure reveals several interesting features in the evolution of underlying deformation mechanisms in both differently oriented specimens. Once the signals

are associated with respective sources, the activity of different deformation mechanisms can be traced separately as it is demonstrated in Figs. 1b and 2b in terms of the cumulative number of class members for both types of single crystals studied. Importantly is that the proposed non-supervised clustering procedure, unlike the conventional k- or c-means algorithms, does not require the user to define the number of derived clusters *a priori*, i.e. it is data-driven, and the number of clusters is determined solely on the basis of statistical differences between incoming signals and their PSDs. Therefore, it is interesting to notice that in the single crystal oriented for basal slip, the ASK procedure returns three clusters corresponding to different AE sources. They have been identified above and correspond to the basal slip, twinning, and the dislocation slip in the twinned fraction. All these mechanisms are represented in Fig. 6. Overall, the AE flow was nearly uniformly composed of the signals caused by dislocation motion with only a small contribution from occasional twins (Fig. 1b shows that the slip-related clusters are by far more representative than that for twins).

Unlike the single crystal oriented for basal slip, the twin-oriented sample behaves in a different way upon loading. According to the ASK analysis Fig. 2b, plastic deformation in the single crystal loaded along the $\langle 11\bar{2}0 \rangle$ axis commences by activation of mechanical twinning, and after of 35 s the dislocation slip comes into play. Despite the coexistence of both deformation mechanisms on the mature stage of straining, the statistical analysis of AE time-series, Fig. 2a, reveals the exponential distribution in the occurrence of inter-arrival times between transients after 120 s. Some "time lag" visible between the crossover point in Fig. 2b and the appearance of green symbols indicating the Poisson-type time series in Fig. 2a is a simple consequence of the statistical procedures involved: the deformation twinning remains very pronounced even after 120 s and the existing memory of the past in the twin-related AE components determines the results of Pierson's goodness-of-fit test until the dislocation slip becomes truly dominating.

Before concluding this work, some of its implications for future research are to be outlined. The main thrust of the present study was to provide solid experimental evidence in support of the hypothesis of the long-term correlations existing between the mechanical twins. The self-exciting nature of these correlations is revealed by the statistical analysis of AE time series at the sub-millisecond and millisecond scale. Not only this suggests that the twins do not evolve independently, but that initiation of a parent twin gives birth to a series of new twins with a locally accelerated rate. An important corollary from this observation is that the temporal twin-twin interaction and correlation has to be taken into account when it comes to modelling the mechanical behaviour of materials that exhibit profuse twinning activity. Within a contemporary purely phenomenological approach, twin boundaries, acting as impenetrable obstacles for dislocation glide, are involved in strain hardening through the so-called dynamic Hall-Petch concept [31, 32],

that bridges the time/strain dependent volume fraction of twins F and the time/strain dependent evolution of the dislocation density. Up to date, the twinning kinetics is most often derived from the Olson-Cohen [33] assumption according to which the twin volume fraction F as a function of strain ε obeys the first-order differential equation $\dfrac{dF(\varepsilon)}{d\varepsilon} = m(1-F)$. Here $(1-F)$ refers to the fraction of the untwinned material where twins may form with the rate determined by the microstructurally sensitive factor m. Although this simple equation captures the ascending trend in $F(\varepsilon)$ to saturation in a general manner, it does not imply any twin-twin interactions. The significance and implications of these interactions on twinning accumulation will be unfolded a dedicated forthcoming publication where appropriate modifications of the existing approach will be proposed and presented in a more elaborate way.

We should also notice that the present results showing that the dislocation slip is a memoryless process at a time scale above a millisecond or so (as resolved by the present signal detector) is in fair agreement with the model and experimental results presented by Vinogradov et al. in [34] where acoustic emission mediated by dislocation slip in pure copper was considered as a continuous Ornstein-Uhlenbeck random process. Unlike the present work, where the burst events can be individually detected, separated from each other and associated with a point process, the low-amplitude AE transients in pure fcc and bcc metals overlap, forming a continuous random noise-like signal. The autocorrelation function of the Ornstein-Uhlenbeck [35] process is exponentially decaying so that the autocorrelation in the high-frequency AE signal caused by dislocation sources approaches zero at the scale of approximately one millisecond, thus signifying a lack of long-term correlation between dislocation avalanches. The millisecond time scale is by far larger than the dislocation mean free flight time, which is usually of the order of few nanoseconds as is commonly estimated by discrete dislocation dynamics simulations [36]. The sub-microsecond time scale of the individual slip line formation has been demonstrated by rapid video imaging in the "classic" experiments by Neuhäuser and co-authors [37, 38], and this time scale agrees reasonably with short low-amplitude transients recorded during dislocation slip line generation during scratch testing of pure copper polycrystals [23].

5. Conclusions

The acoustic emission technique powered by the advanced signal categorization technique was employed to probe the dynamics of dislocation slip and twinning in magnesium single crystals suitably oriented to give preference to one of these two primary deformation modes. It was unambiguously demonstrated that twinning behaved as an intermittent process with the temporal

correlation between the events having a relatively long (of sub-millisecond and millisecond range) memory of the past. As opposes to this, the basal dislocation slip manifested itself as a substantially random process of independent elementary events with no temporal correlations between gliding dislocations or the slip bands emerging to a free surface due to collective dislocation slip along the basal planes.

For the first time, the classification power of the *adaptive sequential k-means* (ASK) algorithm was demonstrated in the model test program that enables predicting the deformation mechanisms with very high confidence and verifying them in direct *in situ* SEM observations.

The signatures of twinning have been revealed by AE in the single crystal "ideally" oriented for basal slip and prompted detailed microscopic observations confirming the appearance of few tiny extension twins. They do not appear to contribute much to the deformation and rather are developed to compensate for the crystal rotation induced by basal slip.

The non-supervised ASK cluster analysis of AE time series is thus proven capable of predictive discrimination between underlying deformation mechanisms, the accurate timing of their activation and evolution.

CRediT author statement.

EA: Methodology, Data curation, Software, Formal analysis, Validation, Visualization, Original draft preparation. **DD:** Data Curation, Visualization, Investigation, Writing - Original Draft. PH: Visualization, Investigation. **PD**: Investigation. **DM:** Project administration, supervision. **AV:** Conceptualization, Methodology, Writing- Reviewing and Editing, Supervision.

Data availability.

The experimental data that support the findings of this study are available from the corresponding author, AV, upon reasonable request.

6. References

[1] R.W. Cahn, Twinned crystals, Advances in Physics 3(12) (1954) 363-445.

[2] J.W. Christian, S. Mahajan, Deformation twinning, Progress in Materials Science 39(1–2) (1995) 1-157.

[3] L. Jiang, M.A. Kumar, I.J. Beyerlein, X. Wang, D. Zhang, C. Wu, C. Cooper, T.J. Rupert, S. Mahajan, E.J. Lavernia, J.M. Schoenung, Twin formation from a twin boundary in Mg during in-situ nanomechanical testing, Materials Science and Engineering: A 759 (2019) 142-153.

[4] A. Vinogradov, E. Agletdinov, D. Merson, Mechanical Twinning is a Correlated Dynamic Process, Scientific Reports 9(1) (2019) 5748.

[5] S. Ni, Y.B. Wang, X.Z. Liao, R.B. Figueiredo, H.Q. Li, S.P. Ringer, T.G. Langdon, Y.T. Zhu, The effect of dislocation density on the interactions between dislocations and twin boundaries in nanocrystalline materials, Acta Materialia 60(6) (2012) 3181-3189.

[6] Y. Chang, D.M. Kochmann, A variational constitutive model for slip-twinning interactions in hcp metals: Application to single- and polycrystalline magnesium, International Journal of Plasticity 73 (2015) 39-61.

[7] K.D. Molodov, T. Al-Samman, D.A. Molodov, Profuse slip transmission across twin boundaries in magnesium, Acta Materialia 124 (2017) 397-409.

[8] F. Wang, C.D. Barrett, R.J. McCabe, H. El Kadiri, L. Capolungo, S.R. Agnew, Dislocation induced twin growth and formation of basal stacking faults in {1012} twins in pure Mg, Acta Materialia 165 (2019) 471-485.

[9] E.W. Kelley, W.F. Hosford, Plane-Strain Compression of Magnesium and Magnesium Alloy Crystals, Transactions of the Metallurgical Society of Aime 242(1) (1968) 5-&.

[10] D. Drozdenko, J. Bohlen, F. Chmelík, P. Lukáč, P. Dobroň, Acoustic emission study on the activity of slip and twin mechanisms during compression testing of magnesium single crystals, Materials Science and Engineering: A 650 (2016) 20-27.

[11] J.F.C. Kingman, Poisson processes, Clarendon Press, Oxford, 1993.

[12] A. Vinogradov, D. Orlov, A. Danyuk, Y. Estrin, Effect of grain size on the mechanisms of plastic deformation in wrought Mg–Zn–Zr alloy revealed by acoustic emission measurements, Acta Materialia 61(6) (2013) 2044-2056.

[13] K. Máthis, G. Csiszár, J. Čapek, J. Gubicza, B. Clausen, P. Lukáš, A. Vinogradov, S.R. Agnew, Effect of the loading mode on the evolution of the deformation mechanisms in randomly textured magnesium polycrystals – Comparison of experimental and modeling results, International Journal of Plasticity 72 (2015) 127-150.

[14] E. Pomponi, A. Vinogradov, A real-time approach to acoustic emission clustering, Mechanical Systems and Signal Proccessing, 40(2) (2013) 791-804.

[15] A. Vinogradov, D. Orlov, A. Danyuk, Y. Estrin, Deformation mechanisms underlying tension–compression asymmetry in magnesium alloy ZK60 revealed by acoustic emission monitoring, Materials Science and Engineering: A 621 (2015) 243-251.

[16] A. Vinogradov, E. Vasilev, D. Merson, Y. Estrin, A phenomenological model of twinning kinetics advanced engineering materials 19(1) (2017) 1600092.

[17] A. Vinogradov, E. Vasilev, M. Linderov, D. Merson, In situ observations of the kinetics of twinning–detwinning and dislocation slip in magnesium, Materials Science and Engineering: A 676 (2016) 351-360.

[18] E. Agletdinov, E. Pomponi, D. Merson, A. Vinogradov, A novel Bayesian approach to acoustic emission data analysis, Ultrasonics 72 (2016) 89-94.

[19] E. Agletdinov, D. Merson, A. Vinogradov, A new method of low amplitude signal detection and its application in acoustic emission, Applied Sciences 10(1) (2019) 73.

[20] C.B. Scruby, H.N.G. Wadley, J.J. Hill, Dynamic elastic displacements at the surface of an elastic half-space due to defect sources, Journal of Physics D: Applied Physics 16(6) (1983) 1069-1083.

[21] A.G. Hawkes, Spectra of some self-exciting and mutually exciting point processes, Biometrika 58(1) (1971) 83-90.

[22] A.G. Hawkes, D. Oakes, A Cluster Process Representation of a Self-Exciting Process, Journal of Applied Probability 11(3) (1974) 493-503.

[23] A. Vinogradov, A.V. Danyuk, D.L. Merson, I.S. Yasnikov, Probing elementary dislocation mechanisms of local plastic deformation by the advanced acoustic emission technique, Scripta Materialia 151 (2018) 53-56.

[24] C.R. Heiple, S.H. Carpenter, Acoustic Emission Produced by Deformation of Metals and Alloys - A review: Part I and II, J. Acoustic Emission. 6(3) (1987) 177-237.

[25] A. Vinogradov, E. Vasilev, M. Seleznev, K. Máthis, D. Orlov, D. Merson, On the limits of acoustic emission detectability for twinning, Materials Letters 183 (2016) 417-419.

[26] A. Chapuis, J.H. Driver, Temperature dependency of slip and twinning in plane strain compressed magnesium single crystals, Acta Materialia 59(5) (2011) 1986-1994.

[27] K.D. Molodov, T. Al-Samman, D.A. Molodov, G. Gottstein, On the role of anomalous twinning in the plasticity of magnesium, Acta Materialia 103 (2016) 711-723.

[28] P.G. Partridge, The crystallography and deformation modes of hexagonal close-packed metals, Metallurgical Reviews 12(1) (1967) 169-194.

[29] M.R. Barnett, Twinning and the ductility of magnesium alloys. Part I: "Tension" twins, Materials Science and Engineering A 464(1-2) (2007) 1-7.

[30] G.S. Kim, Small volume investigation of slip and twinning in magnesium single crystals, Ph.D. Thesis,. Universite de Grenoble, Grenoble, France, 2011.

[31] O. Bouaziz, N. Guelton, Modelling of TWIP effect on work-hardening, Materials Science and Engineering: A 319–321(0) (2001) 246-249.

[32] S. Allain, J.P. Chateau, O. Bouaziz, A physical model of the twinning-induced plasticity effect in a high manganese austenitic steel, Materials Science and Engineering: A 387–389(0) (2004) 143-147.

[33] G.B. Olson, M. Cohen, Kinetics of strain-induced martensitic nucleation, Metallurgical Transactions A 6(4) (1975) 791-795.

[34] A. Vinogradov, I.S. Yasnikov, Y. Estrin, Stochastic dislocation kinetics and fractal structures in deforming metals probed by acoustic emission and surface topography measurements, Journal of Applied Physics 115(23) (2014) 233506

[35] G.E. Uhlenbeck, L.S. Ornstein, On the Theory of the Brownian Motion, Physical Review 36(5) (1930) 823-841.

[36] M. Hiratani, H.M. Zbib, Stochastic dislocation dynamics for dislocation-defects interaction: A Multiscale Modeling Approach, Journal of Engineering Materials and Technology 124(3) (2002) 335-341.

[37] M. Kügler, A. Hampel, H. Neuhäuser, Slip line kinetics during deformation of Cu-Al single and polycrystals, Physica Status Solidi (A) Applied Research 175(2) (1999) 513-526.

[38] U. Hoffmann, A. Hampel, H. Neuhäuser, In situ optical microscopic recording of slip line development during plastic deformation of Cu-15at%Al single crystals with high resolution - Estimation of dislocation velocities, Journal of Microscopy 203(1) (2001) 108-118.

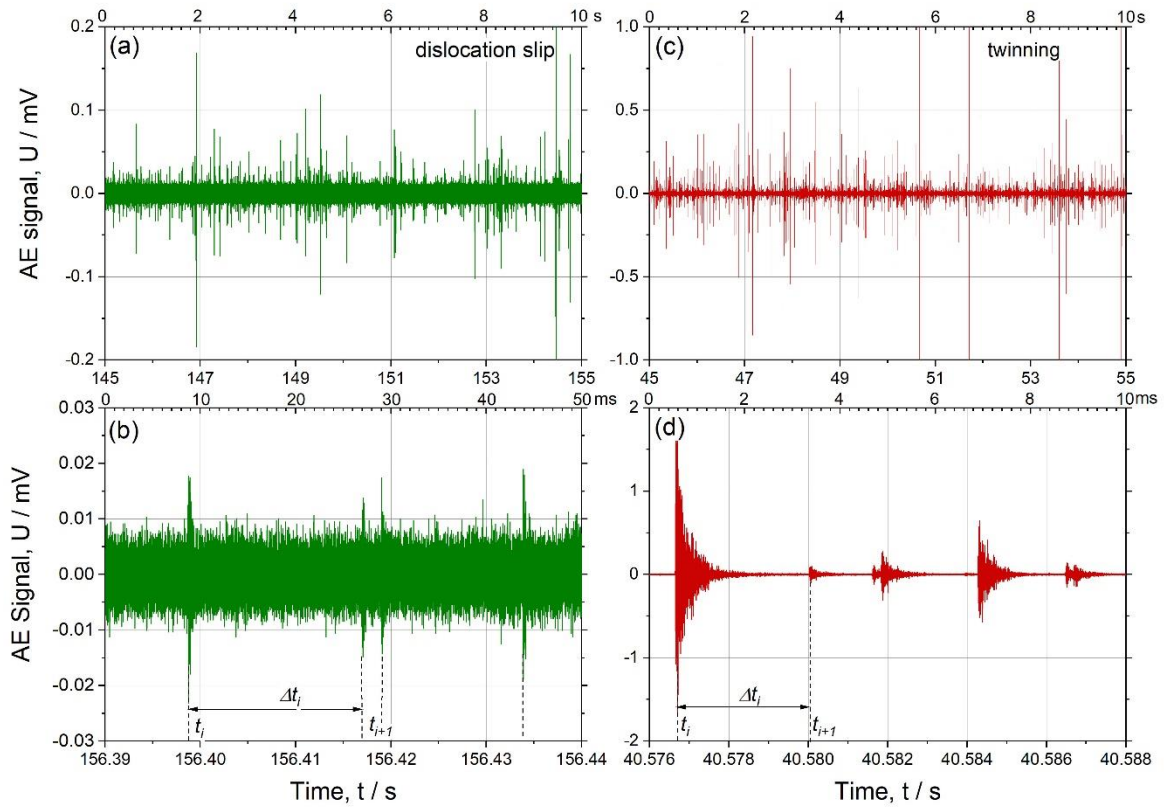**Figure 1.** Typical fragments (sectioned from the raw AE streaming data with different time scales) of AE time series exemplifying the AE response dominated by dislocation slip (green) (a, b) and twinning (red) (c, d) in the magnesium single crystal deformed along the $\langle 11\bar{2}0 \rangle$ axis, c.f. Fig. 3 and refer to the section *Results* for details.
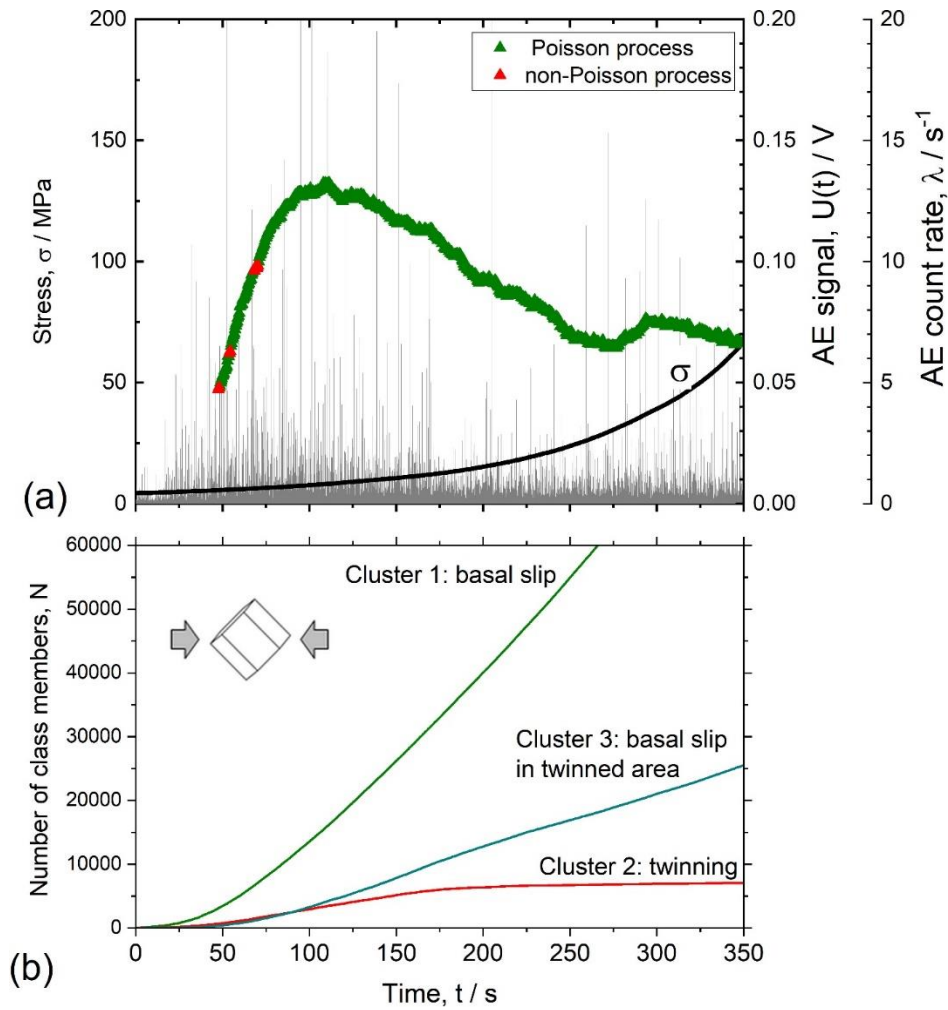
Figure 2. AE activity in the Mg single crystal deformed along the $\langle 11\bar{2}2 \rangle$ axis, promoting the basal slip: (a) AE count rate and raw AE signal correlated with the deformation curve; (b) non-supervised cluster analysis of AE signal.
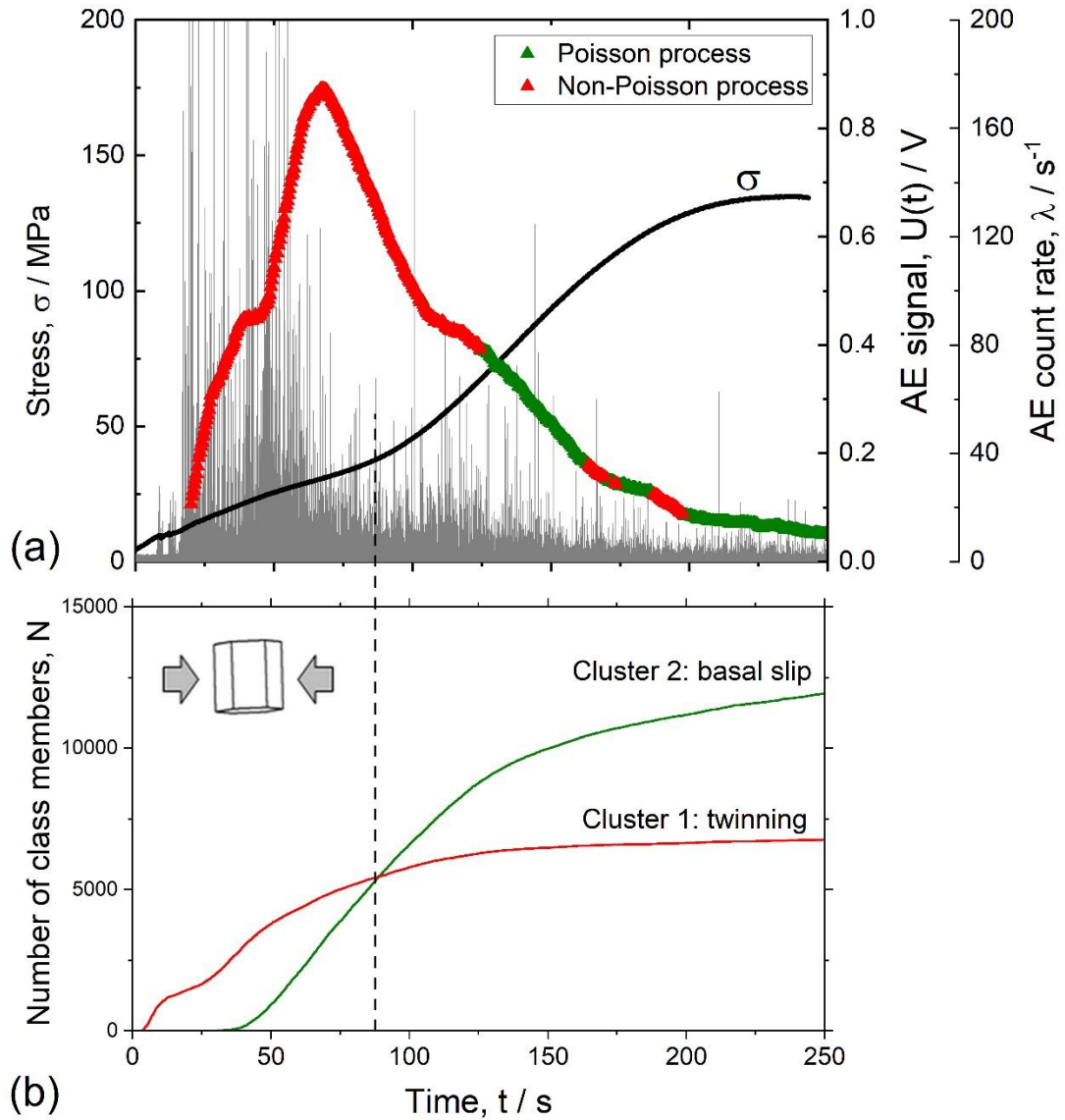
Figure 3. AE activity λ (triangles) in the Mg single crystal deformed along the $\langle 11\bar{2}0 \rangle$ axis, promoting twinning: (a) AE count rate and raw AE signal correlated with deformation curve; (b) non-supervised cluster analysis of AE signal. The dashed line indicates a cross-over between the two primary deformation modes, which coincides with the inflexion point on the loading diagram.
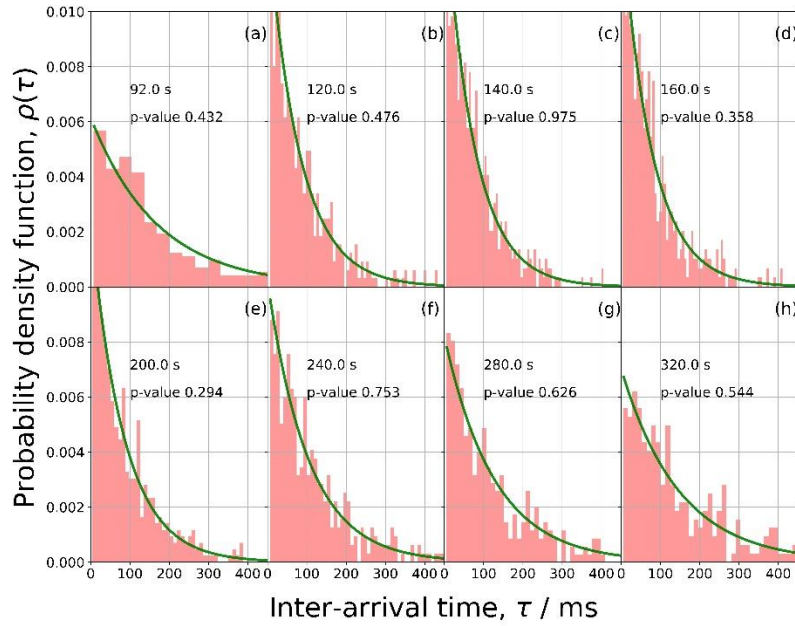
Figure 4. The evolution of the distribution function of time intervals between successive events in the AE time series corresponding to Fig. 2. Time marks corresponding to some fragments are shown in each sub-figure.
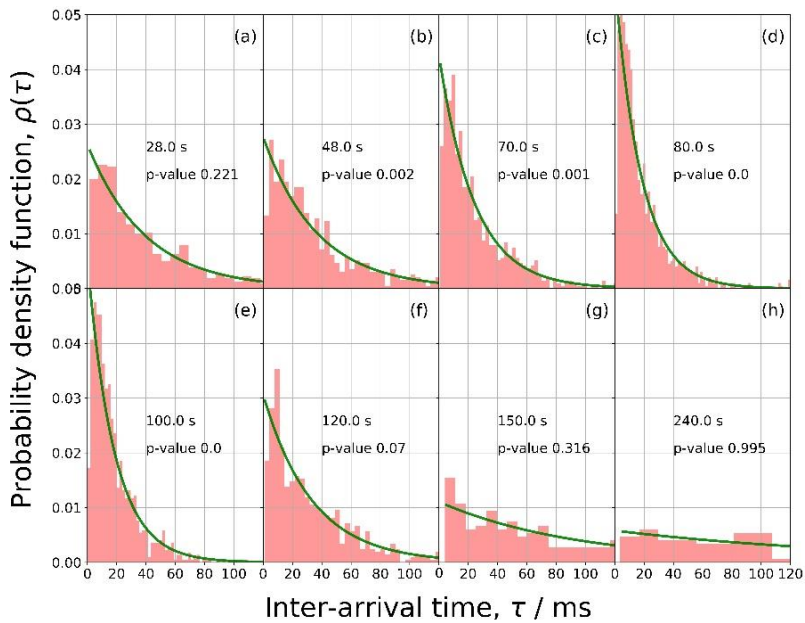

Figure 5. The evolution of the distribution function of time intervals between successive events in the AE time series corresponding to Fig. 3. Different time intervals $j \in [1, K]$ are shown in each sub-figure.
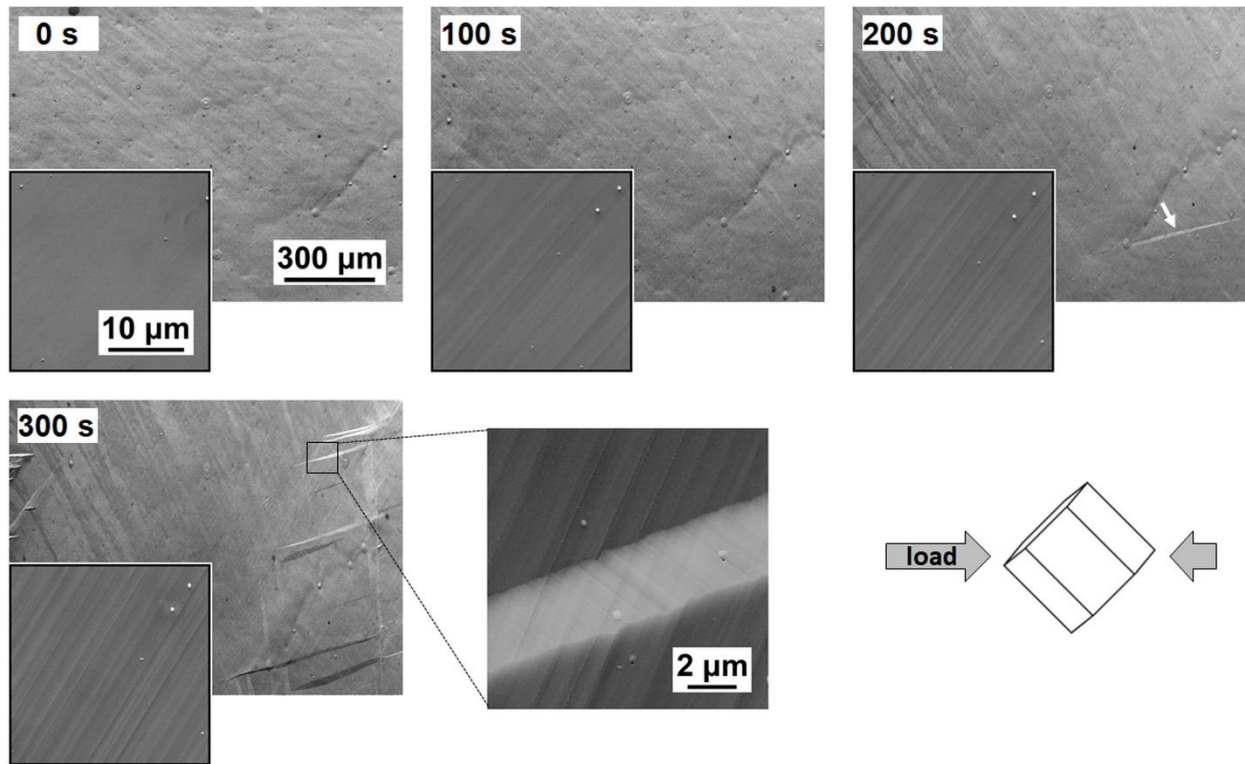
Fig. 6. A sequence of SEM images showing the microstructure evolution observed *in-situ* during compressive loading of the Mg single crystal along the $\langle 11\bar{2}2 \rangle$ axis favorable for the basal <a> dislocation slip. All images refer to the same surface fragment: visible changes in the grey contrast are due to the SEM settings and the variation of the working distance during loading. The appearance of the tiny twin is highlighted by the white arrow. The inset to the "300 s" image showing the magnified fragment of the deformation twin reveals the traces of the secondary slip in the twinned region.
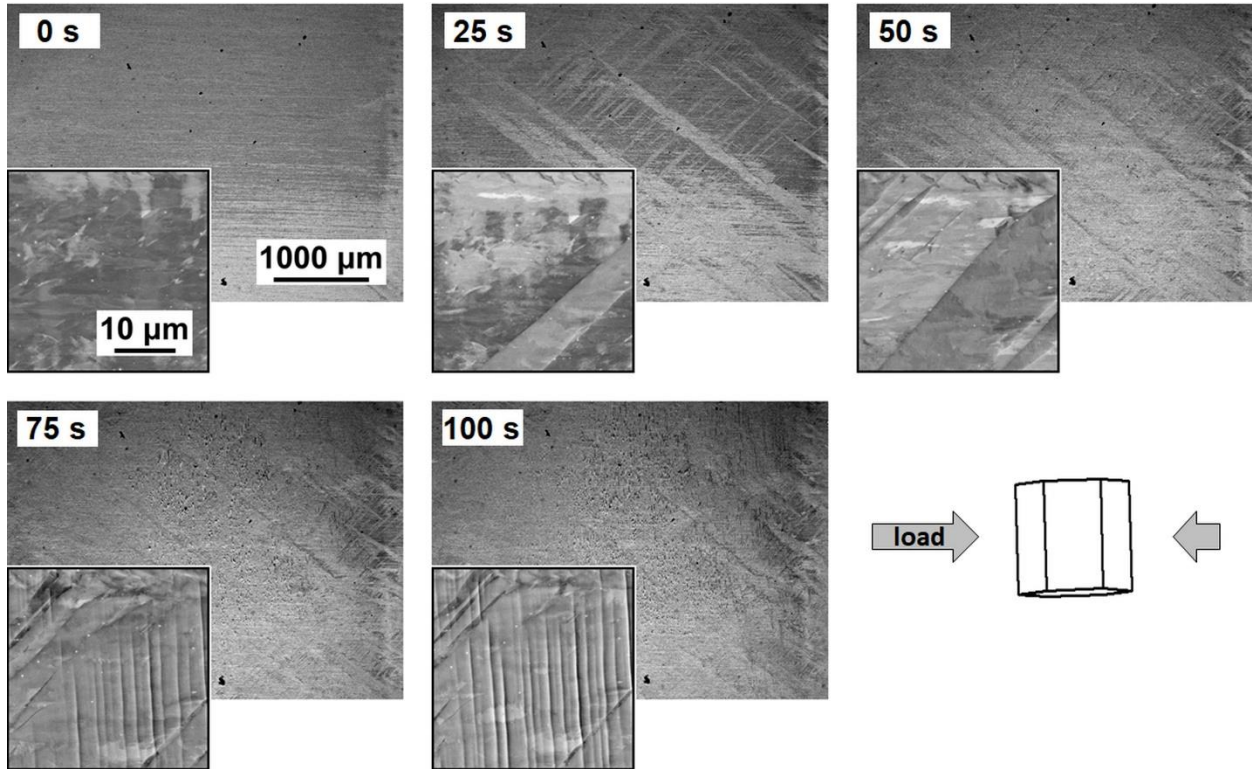
Fig. 7. A sequence of SEM images showing the microstructure evolution observed *in-situ* during compressive loading of the Mg single crystal along the ⟨11$\bar{2}$0⟩ axis favourable for {10$\bar{1}$2} extension twinning.